Geophysical Research Letters

RESEARCH LETTER
10.1029/2021GL094691

Global Survey of the MJO and Extreme Precipitation

Carl J. Schreck III[1]

[1]Cooperative Institute for Satellite Earth System Studies (CISESS), North Carolina Institute for Climate Studies (NCICS), North Carolina State University (NCSU), Raleigh, NC, USA

Key Points:

- The Madden-Julian Oscillation (MJO) significantly affects extreme precipitation events around the globe and during all seasons
- The modulation of extreme precipitation by the MJO is often driven more by its low-level winds than its convective circulation
- These results could be leveraged for valuable subseasonal forecasts of extreme events to farmers and water resource managers

Supporting Information:

Supporting Information may be found in the online version of this article.

Correspondence to:

C. J. Schreck,
carl_schreck@ncsu.edu

Citation:

Schreck, C. J., III. (2021). Global survey of the MJO and extreme precipitation. *Geophysical Research Letters*, *48*, e2021GL094691. https://doi.org/10.1029/2021GL094691

Received 4 JUN 2021
Accepted 23 SEP 2021

Abstract This study examines the modulation of land-based extreme precipitation around the globe by the Madden-Julian Oscillation (MJO). The upper-level convergent phase of the MJO inhibits extreme events over most regions but enhancement in other phases falls in three categories. Over Brazil, Southeast Asia, and Australia, 2-year rainfall events are most common near the core of the upper-level divergence as expected. For most other regions in the tropics and subtropics, the extreme events occur along the periphery of the MJO's envelope. Previous regional studies suggest these extremes are driven by the MJO's low-level circulation either advecting moisture or interacting with orography rather than directly increasing the vertical convection. Finally, extratropical extreme events are more likely associated with the MJO's impact on extratropical wave trains or tropical cyclones. Given the increasing skill of numerical models for predicting the MJO, these results could lead to subseasonal forecasts of extreme events.

Plain Language Summary This study shows how the Madden-Julian Oscillation (MJO) affects heavy rainfall events everywhere. The dry phase of the MJO prevents extreme rainfall as expected. However, the extreme events in the wet phase are probably enhanced in one of three ways. Over Brazil, Southeast Asia, and Australia, the extreme events are closely tied to the MJO's primary enhanced rainfall. Across other parts of the tropics and subtropics, they are driven more by the MJO's low-level winds. These winds either transport moisture from nearby oceans or increase rainfall through upslope winds over mountains. Finally, the extremes in the extratropics are driven more by the MJO's effects on other systems like extratropical waves and tropical cyclones. State-of-the-art models can predict the MJO's movements 2–3 weeks in advance. A forecaster could use those predictions to anticipate extreme events based on the results of this study. Such a forecast might give farmers and water resource managers the time they need to prepare for those events.

1. Introduction

The Madden-Julian Oscillation (MJO) is the dominant mode of subseasonal tropical variability (Zhang, 2005; Zhang et al., 2013). Because of its intense modulation of tropical convection, it affects weather patterns and extreme events around the globe (Zhang, 2013). These effects include heat waves, cold waves, tropical cyclones, fires, and extreme rainfall events. The MJO lies at the subseasonal interface between weather and climate, so these effects can be critical for long-range forecasts. This study will examine the MJO's modulation of land-based extreme rainfall around the globe.

Numerous studies have examined the MJO's effects on precipitation extremes, but most of these have been regional in scale. For example, flooding events in Sumatra (in the heart of the MJO's convective variability) tend to initiate when the MJO is over the Indian Ocean (phases 2–3) (Baranowski et al., 2020). The MJO's winds also interact strongly with the large topography and moisture availability over South America. When the MJO's convection is over the Central Pacific and Western Hemisphere (phases 8–1), an enhanced South Atlantic Convergence Zone (SACZ) can lead to extreme rainfall over northeastern Brazil (Carvalho et al., 2004; Grimm, 2019; Hirata & Grimm, 2016; Shimizu et al., 2017).

The MJO's teleconnections also affect extreme precipitation outside the tropics. For example, extreme precipitation events in the United States are significantly more likely when the MJO is active (particularly over the Indian Ocean) than when it is not (Jones & Carvalho, 2012). The MJO modulates drivers for extreme rainfall like atmospheric rivers (Baggett et al., 2017; Mundhenk et al., 2018; Ralph et al., 2011) and tropical cyclones (Barrett & Leslie, 2009; Klotzbach, 2010; Kossin et al., 2010; Maloney & Hartmann, 2000; Mo, 2000). When the MJO is over the Western Hemisphere (phases 8–1), it also significantly enhances

extreme precipitation over arid Southwest Asia (Barlow et al., 2005; Hoell et al., 2018; Nazemosadat & Shahgholian, 2017; Nazemosadat et al., 2021).

Despite these regional studies, Jones et al. (2004) provided the only global study of precipitation extremes with the MJO. These extremes broadly followed the MJO's convective envelope and included many of the regional examples above. Aggregated globally, they found that extreme events occurred 40% more often when the MJO was active than when it was not. Jones et al. (2004) also demonstrated the ability of a general circulation model (GCM) to replicate these broad patterns.

The current study provides a more complete picture of the MJO's global effects on the most societally relevant extreme rainfall events. It builds upon Jones et al. (2004) in several key ways. Most importantly, this study uses a higher definition of extreme events. Jones et al. (2004) used the 75th percentile of raining pentads, which ensured a large sample size but diluted the societal impact. The current study uses 2-year events, which are much more extreme (>99.5th percentile) and more likely to cause flooding and other societal impacts (Leopold, 1968). This study will also explore all seasons whereas Jones et al. (2004) only examined November–April. Finally, they used Global Precipitation Climatology Project (GPCP) data, which are 5-day means on a coarse 2.5° grid. This study will leverage the new NASA IMERG (Integrated Multi-satellitE Retrievals for the Global Precipitation Measurement Mission) data set (Huffman et al., 2015, 2019), which is a daily 0.1° grid. This fine resolution allows us to exclude precipitation over the oceans where it is less societally relevant.

2. Data

The NASA IMERG data are used for June 1, 2000–June 30, 2020. Only data over land 60°S–60°N are used here. Satellite-based precipitation data sets like IMERG notoriously underestimate the magnitudes of extreme precipitation events relative to gauge-based measurements (Prat & Nelson, 2020). However, IMERG is particularly good at estimating events with short return-periods like the 2-year events examined here (Fang et al., 2019). Using the same data set to define and detect the extreme events also mitigates the underestimation since the absolute amplitude of the event is not relevant.

MJO phases are determined using the Wheeler and Hendon (2004) index. Only days when the MJO amplitude is greater than one standard deviation are used. Velocity potential anomalies at 200 hPa are taken from the Climate Forecast System Reanalysis (CFSR) (Saha et al., 2010) for 1998–2010 and the related Climate Forecast System v2 (CFSv2) operational analyses (Saha et al., 2014) for 2011–2020. These are plotted by the MJO phase to illustrate the broader MJO circulation.

3. Methods

3.1. Defining Extreme Events

Following Bosma et al. (2020), extreme rainfall events are defined herein as 2-year events. The 2-year event threshold is calculated by determining the annual maximum at each gridpoint for each year during 2001–2019 (omitting 2000 and 2020, which only had partial data). The median of these 19 annual maxima is the 2-year precipitation intensity at that location. Daily rainfall events are examined here, but similar results were obtained for 5-day events (not shown). Since a 2-year event occurs on average once every 730 days, it represents approximately the wettest 0.14% of days (including those without rain), which is much higher than other typical definitions for extreme events like the 75th–95th percentiles.

A 2-year event is advantageous because it is extreme enough to produce societal impacts (Leopold, 1968). However, it is statistically stable since its calculation does not depend on any parameterized extreme value analysis. It is also more useful from a communication standpoint than concepts like a 10-year or 100-year flood, which can be confusing to users who are more likely to have a frame of reference for a 2-year event.

Figure 1a maps the thresholds for a 2-year event, which generally mirror the distribution of mean precipitation (not shown). In the wettest tropical regions, the 2-year event intensity can exceed 200 mm while it

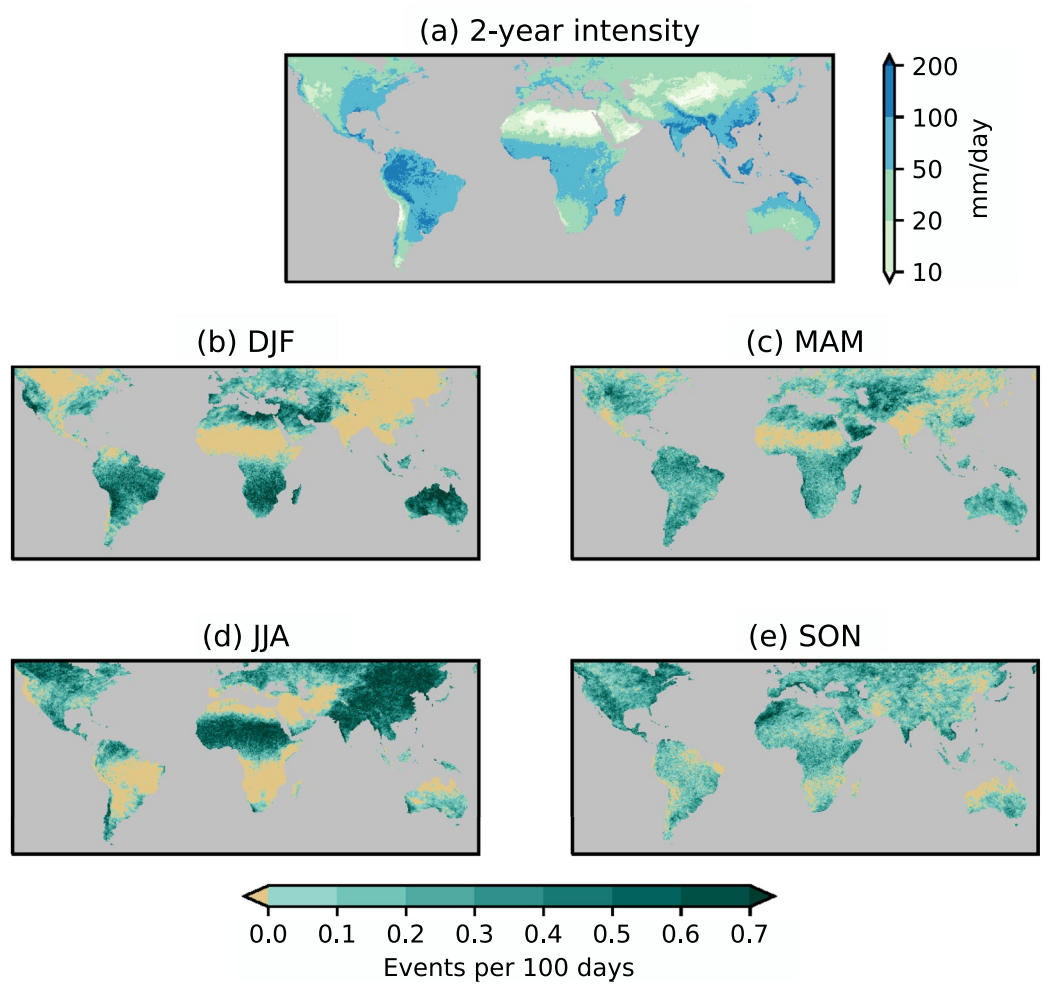

Figure 1. (a) 2-year event intensity threshold. Number of 2-year events by season: (b) December–February, (c) March–May, (d) June–August, and (e) September–November.

can be as low as 10–20 mm day^{-1} in deserts. However, the rarity of precipitation in arid areas means that even these small amounts can have societal impacts (Hoell et al., 2018; Nazemosadat & Shahgholian, 2017)

Extreme rainfall events have a strong seasonality (Figures 1b–1e), which also follows the annual cycle of mean precipitation (not shown). In most regions, 2-year events only happen during one or two seasons. Over the Sahel and East Asia, for example, they happen almost exclusively during JJA. If the frequency of these events during other seasons is zero, then the JJA frequency would be around 0.5 events per 100 days or once every other JJA.

3.2. Statistical Significance

The counts per phase are normalized to the number of events per 100 days. Statistical significance is evaluated using the cumulative distribution function for a binomial distribution. A point is considered significant (green pixels in Figures 2–5) if there is less than a 5% chance that the observed number of events would occur within the number of days in a particular phase given the climatological probability (Figures 1b–1e).

For example, the MJO spent 268 days in phases 2–3 during December–February (DJF) (Figure 2a). If the climatological frequency at a gridpoint was exactly one in 2 years (0.14 events per 100 days), then that

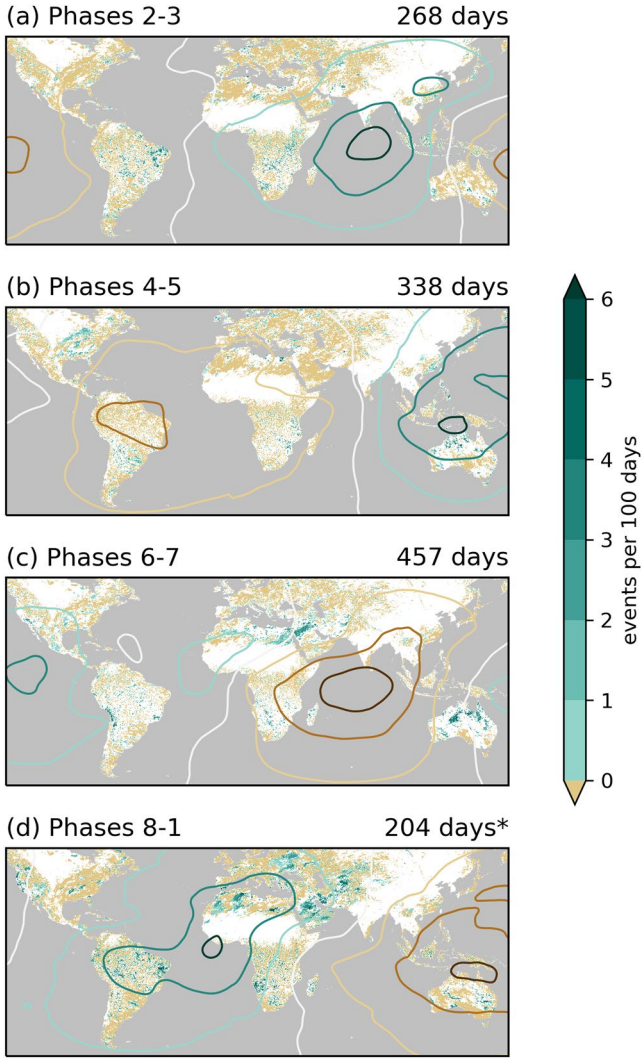

Figure 2. Normalized number of events for December–February in Madden-Julian Oscillation phases (a) 2–3, (b) 4–5, (c) 6–7, and (d) 8–1. White areas are not significantly greater than normal, brown areas have zero events during those phases, and green areas have significantly more events than normal. Contours illustrate the 200-hPa velocity potential anomalies contoured every 2×10^6 m^2 s^{-1} with negative (divergent) values in green and positive (convergent) values in brown. Sample number of days for that phase are in the upper right with a * denoting maps that passed field significance at the 0.10 level (Wilks, 2006).

gridpoint would be significantly above climatology (green) if it had at least two events in the 268 days (0.75 events per 100 days). Brown pixels are those for which the climatological probability is nonzero but no events were observed for that phase. White pixels are areas where either the number of events is not significantly different from climatology or no events occur during that season regardless of the MJO (zero climatology).

Each global map has around 300,000 nonzero points. This large number of hypothesis tests raises the potential for false discoveries. In each map, around 20% of the nonzero points pass the 0.05 local significance level. This large fraction is virtually impossible by random chance, although this counting method can be too permissive for correlated data sets (Wilks, 2006). An alternative is the "false discovery rate" (FDR), which weights each p-value by its rank relative to the total number of tests. Maps with at least one point passing the 0.10 level for the FDR are denoted with an * next to the sample size to indicate field significance (e.g., Figure 2d).

4. Results

4.1. December–February (DJF)

Figure 2 illustrates the MJO's impacts on 2-year rainfall events for DJF. It shows the number of events that occur at each IMERG grid point by the MJO phase. Extreme rainfall events are rare by definition, and the IMERG data have 0.1° horizontal resolution. As a result, the maps of 2-year events by the MJO phase are noisy with areas of significant increases (green) interspersed with those of no significant change (white) or even no events at all (brown).

During phases 2–3 (Figure 2a), the MJO's upper-level divergence is centered over the Indian Ocean, but the extreme events occur along its periphery over East Africa and the western Maritime Continent (Figure S1a in Supporting Information S1). Eastern Brazil also experiences enhanced extreme rainfall in phases 2–3, but these are more widespread when the upper-level divergence is closer in phases 8–1 (Figures 2d and S2d in Supporting Information S1).

During phases 4–5 (Figures 2b and S1b in Supporting Information S1), the tropical enhancement of extreme rainfall shifts eastward to the Philippines and northern Australia. Jones et al. (2004, their Figure 6) found widespread enhancement of extreme rainfall in the seas around Indonesia in phases 4–5, but the higher spatial resolution of the IMERG data more clearly demonstrates that the impact is more limited over the islands during these phases, consistent with Baranowski et al. (2020).

The enhancement over northeastern Australia becomes stronger in phases 6–7 (Figures 2b and S1c in Supporting Information S1) even though the upper-level divergence is over the Pacific. The Australian signal is stronger than that found by Jones et al. (2004), who also found the enhancement to be more focused on phases 4–5. The Central Andes also experience enhanced extreme rainfall on the eastern edge of the MJO's envelope during these phases (Figure S2b in Supporting Information S1). In phases 8–1 (Figure 2d), the largest tropical enhancement is over Brazil, which is within the MJO's divergent upper-level circulation.

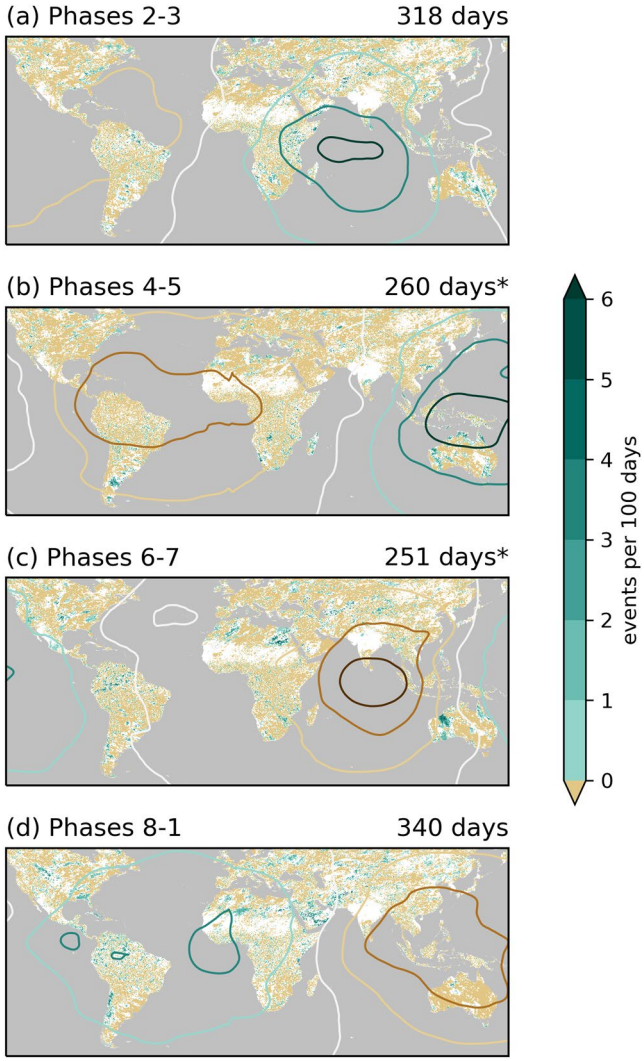

Figure 3. As in Figure 2 but for March–May.

In the subtropics, the MJO's modulation of extreme rainfall is particularly strong around the Mediterranean and Southwest Asia. Phases 6–7 demonstrate a strong subtropical enhancement over Egypt, northern Saudi Arabia, and Iraq (Figure S3a in Supporting Information S1). It becomes even more widespread across the region in phases 8–1 (Figure S3d in Supporting Information S1) as the MJO's upper-level divergence over Africa becomes stronger. The threshold for a 2-year event is much lower in these arid regions (Figure 1a), which could make these events easier to produce than in wetter regions. Satellite-based precipitation estimates are also particularly uncertain over these arid regions (Fang et al., 2019; Prat & Nelson, 2020). However, neither of these uncertainties could explain the coherent evolution of these events with the MJO phase, which are consistent with Jones et al. (2004) and previous studies of the region (Barlow et al., 2005; Hoell et al., 2018; Mansouri et al., 2021; Nazemosadat & Shahgholian, 2017; Nazemosadat et al., 2021). However, none of these previous studies noted the signal over northern Africa.

In addition to the tropical and subtropical signals, Figure 2 also shows signals that are less directly tied to the MJO's convective envelope. For example, phases 4–5 show an enhancement near the central United States, which could be associated with a northward shift in the jet during these phases (Becker et al., 2011). Phases 8-1 bring increased events to the U.S. West Coast, which is consistent with impacts on atmospheric rivers there (Baggett et al., 2017; Mundhenk et al., 2018; Ralph et al., 2011). Similar changes in the extratropical wavetrains lead to enhanced extreme rainfall near the Parana-La Plata Basin of South America during phases 4–5 as well (Figure S2b in Supporting Information S1) (Grimm, 2019; Hirata & Grimm, 2016).

4.2. March–May (MAM)

Figure 3 repeats the analysis for MAM when most regions experience fewer extreme precipitation events (Figure 1c). North Africa and Southwest Asia experience a similar modulation by the MJO between DJF and MAM with an enhancement in phases 6–7 and 8–1 (Figures 3c and 3d). East Africa is also generally similar between these seasons with the largest enhancement in phases 2–3 and the greatest suppression in phases 6–7.

Australia, on the other hand, has a much less organized pattern during MAM, in part because these events are less common during those months (Figure 1c). Australia experiences 2-year events over scattered regions during all the MJO phases with the notable exception of phases 8–1 when they are rare. The clearest signals over South America during MAM are an enhancement over southern Argentina in phases 4–5 (Figure 3b) and central Chile in phases 8–1 (Figure 3d).

4.3. June–August (JJA)

During JJA, 2-year events are primarily concentrated near the Sahel and East Asia (Figure 1d). Two-year events are suppressed over the Sahel within upper-level convergent (brown contours, convectively suppressed) phases of the MJO, particularly phases 4–5 (Figure S4b in Supporting Information S1). Extreme events are also inhibited over Central America during these phases consistent with Barrett and Esquivel Longoria (2013). They are most frequent over the Sahel during phases 2–3 when the MJO is over the Indian

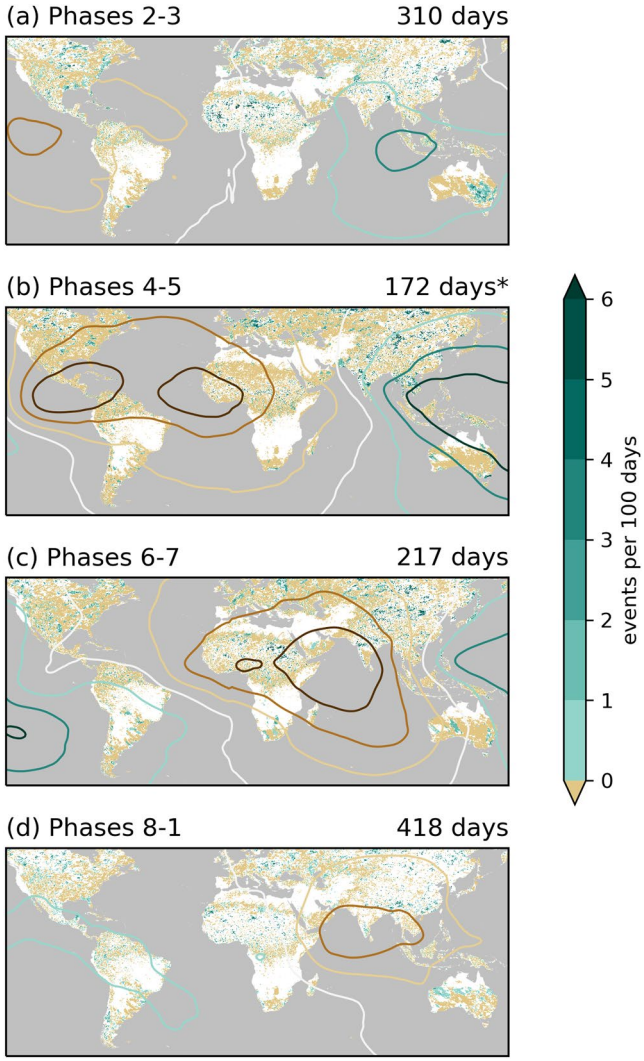

Figure 4. As in Figure 2 but for June–August.

Ocean, but many areas are not significantly different from climatology in phases 8–1 or 2–3. The MJO also enhances extreme precipitation in central Chile during phase 8–1 as in Barrett et al. (2012).

The MJO's modulation of extreme rainfall is less organized over East Asia (Figures 4 and S5 in Supporting Information S1). The strongest enhancement occurs during phases 4–5 when the upper-level divergence is closest (Figure S5b in Supporting Information S1). Two-year events are particularly frequent in these phases for southern India, Southeast Asia, northern China, and the coast of the Yellow Sea. However, the enhanced regions are surround by large areas that received no 2-year events during these phases.

4.4. September–November (SON)

The global frequency of 2-year events is more uniform during SON. Most of the global land experiences at least some extreme precipitation during SON, but <5% of gridpoints exceed 0.5 events per 100 days. The most active regions for these events during SON are North America, northwestern Africa, southern Europe, southern India, and Southeast Asia. The events over the southeastern U.S. are significantly more frequent during phases 2–3 (Figures 5a and S6a in Supporting Information S1) and rare during phases 6–7 (Figure 5c and S6c in Supporting Information S1). These patterns align well with the MJO's modulation of Atlantic tropical cyclone activity (Barrett & Leslie, 2009; Klotzbach, 2010; Kossin et al., 2010), which is the dominant driver of extreme precipitation for that region and season (Kunkel et al., 2010; Prat & Nelson, 2013a, 2013b, 2016).

The MJO relationship is weaker over northwestern Africa and southern Europe with enhanced 2-year events during phases 2–3 and again in phases 6–7 (Figures 5a and 5c). However, they are broadly suppressed in those regions during phases 8–1. Southern India and Southeast Asia predominantly experience these during phases 4–5 in SON (Figure 5b).

5. Conclusions

This study leverages the unprecedently high spatial resolution and global coverage of the NASA IMERG precipitation data to examine the MJO's impacts on extreme rainfall around the globe. Most studies of the MJO and precipitation extremes have focused on individual regions. Jones et al. (2004) examined the global impacts of the MJO during November–May. The current study extends those results in several key ways: examining other seasons, using higher spatial resolution data, focusing on land areas, and using a higher definition of extreme events (2-year events).

Jones et al. (2004) found that the extreme events generally follow the MJO's convective envelope in the tropics. However, those results were driven primarily by events over the ocean. The higher spatial resolution of IMERG allows us to focus on land where the societal impacts are greatest. As in Jones et al. (2004), Australia and Brazil both experience extreme precipitation most frequently when they are near the center of the MJO's convective envelope. In most other parts of the tropics and subtropics, however, the extreme events occur on the periphery of the upper-level divergence. Based on previous regional studies, these extreme events are often associated with changes in moisture transport by the MJO's low-level winds. For example, the extreme precipitation over Southwest Asia during phases 8–1 is associated with enhanced moisture flux from the Arabian Sea in association with the MJO (Barlow et al., 2005; Hoell et al., 2018; Nazemosadat & Shahgholian, 2017)

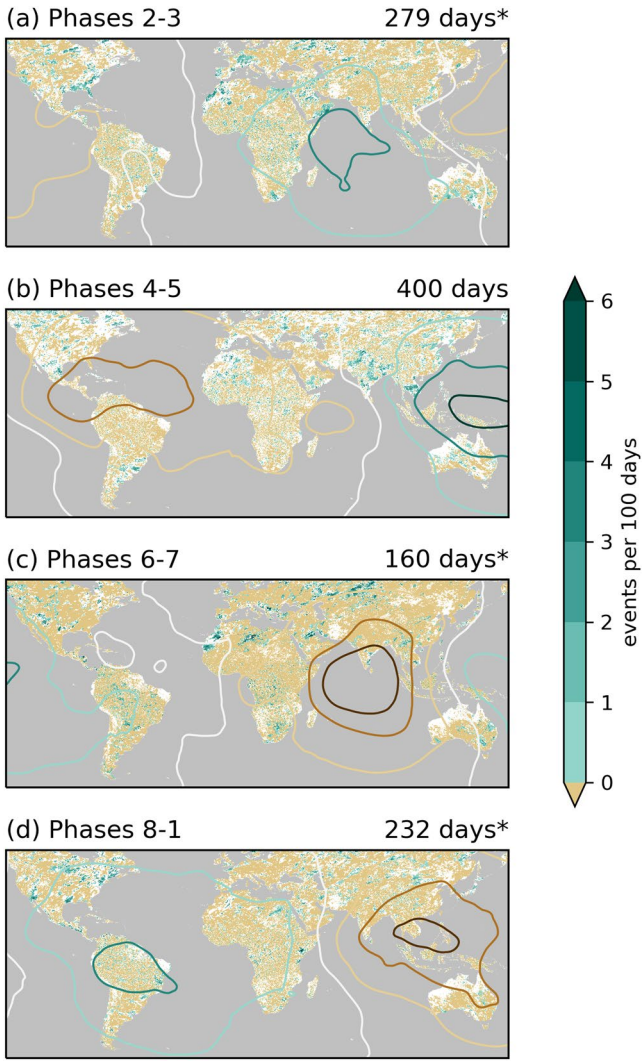

Figure 5. As in Figure 2 but for September–November.

In the extratropics, the modulation of extreme events is less likely to be tied to the MJO's primary circulation. For example, the MJO's modulation of Atlantic tropical cyclone activity leads to variations in extreme rainfall over the Southeast during SON. Similarly, the MJO modulates the PNA during the winter (Riddle et al., 2013) which in turn modulates the frequency of atmospheric rivers and extreme precipitation along the West Coast of North America (Baggett et al., 2017; Mundhenk et al., 2018). It can take 1–2 weeks for the MJO's tropical forcing to result in these extratropical responses (Baxter et al., 2014; Matthews et al., 2004), so some of their effects may have been diluted in this study by examining only instantaneous phases in the current study.

Jones et al. (2004) demonstrated the ability of a global circulation model with fixed SSTs to replicate many of these relationships. Numerical models can now skillfully forecast the MJO out to 3 weeks (Kim et al., 2014; Vitart & Molteni, 2010), so the results of this study may have significant value for subseasonal prediction of extreme rainfall. It would be valuable to examine how well they can now predict its extreme rainfall events. The results could be leveraged to develop subseasonal forecasts of extreme event probability, which could prove invaluable to farmers and water resource managers.

Finally, it is well-established that climate change is making extreme rainfall events more common (IPCC, 2021). However, it is not clear how that trend would affect the relationship between the MJO and extreme events. Would events become more common in all phases, even those currently inhibited? Or would they simply become more common in the phases that already favor them? Additional modeling should examine these questions.

Data Availability Statement

All data used in this manuscript are publicly available. The NASA IMERG data may be obtained from https://doi.org/10.5067/GPM/IMERGDF/DAY/06. The MJO index was obtained from http://www.bom.gov.au/climate/mjo/. CFSv2 data were obtained from https://rda.ucar.edu/datasets/ds094.0/ and the CFSR from https://rda.ucar.edu/datasets/ds093.0/.

Acknowledgments
This project was supported by NASA grant NNX16AE33G, NOAA grant NA18OAR4310297, and by NOAA through the Cooperative Institute for Satellite Earth System Studies under Cooperative Agreement NA19NES4320002.

References

Baggett, C. F., Barnes, E. A., Maloney, E. D., & Mundhenk, B. D. (2017). Advancing atmospheric river forecasts into subseasonal-to-seasonal time scales. *Geophysical Research Letters*, *44*(14), 7528–7536. https://doi.org/10.1002/2017GL074434

Baranowski, D. B., Flatau, M. K., Flatau, P. J., Karnawati, D., Barabasz, K., Labuz, M., et al. (2020). Social-media and newspaper reports reveal large-scale meteorological drivers of floods on Sumatra. *Nature Communications*, *11*(1), 2503. https://doi.org/10.1038/s41467-020-16171-2

Barlow, M., Wheeler, M., Lyon, B., & Cullen, H. (2005). Modulation of daily precipitation over Southwest Asia by the Madden–Julian Oscillation. *Monthly Weather Review*, *133*(12), 3579–3594. https://doi.org/10.1175/MWR3026.1

Barrett, B. S., Carrasco, J. F., & Testino, A. P. (2012). Madden–Julian Oscillation (MJO) modulation of atmospheric circulation and Chilean winter precipitation. *Journal of Climate*, *25*(5), 1678–1688. https://doi.org/10.1175/JCLI-D-11-00216.1

Barrett, B. S., & Esquivel Longoria, M. I. (2013). Variability of precipitation and temperature in Guanajuato, Mexico. *Atmósfera*, *26*(4), 521–536. https://doi.org/10.1016/S0187-6236(13)71093-2

Barrett, B. S., & Leslie, L. M. (2009). Links between tropical cyclone activity and Madden–Julian Oscillation phase in the North Atlantic and Northeast Pacific basins. *Monthly Weather Review*, *137*(2), 727–744. https://doi.org/10.1175/2008MWR2602.1

Baxter, S., Weaver, S., Gottschalck, J., & Xue, Y. (2014). Pentad evolution of wintertime impacts of the Madden–Julian Oscillation over the Contiguous United States. *Journal of Climate*, *27*(19), 7356–7367. https://doi.org/10.1175/JCLI-D-14-00105.1

Becker, E. J., Berbery, E. H., & Higgins, R. W. (2011). Modulation of cold-season U.S. daily precipitation by the Madden–Julian Oscillation. *Journal of Climate*, *24*, 5157–5166. https://doi.org/10.1175/2011JCLI4018.1

Bosma, C. D., Wright, D. B., Nguyen, P., Kossin, J. P., Herndon, D. C., & Shepherd, J. M. (2020). An intuitive metric to quantify and communicate tropical cyclone rainfall hazard. *Bulletin of the American Meteorological Society*, *101*(2), E206–E220. https://doi.org/10.1175/BAMS-D-19-0075.1

Carvalho, L. M. V., Jones, C., & Liebmann, B. (2004). The South Atlantic Convergence Zone: Intensity, form, persistence, and relationships with intraseasonal to interannual activity and extreme rainfall. *Journal of Climate*, *17*, 21. https://doi.org/10.1175/1520-0442(2004)017<0088:tsaczi>2.0.co;2

Fang, J., Yang, W., Luan, Y., Du, J., Lin, A., & Zhao, L. (2019). Evaluation of the TRMM 3B42 and GPM IMERG products for extreme precipitation analysis over China. *Atmospheric Research*, *223*, 24–38. https://doi.org/10.1016/j.atmosres.2019.03.001

Grimm, A. M. (2019). Madden–Julian Oscillation impacts on South American summer monsoon season: Precipitation anomalies, extreme events, teleconnections, and role in the MJO cycle. *Climate Dynamics*, *53*(1–2), 907–932. https://doi.org/10.1007/s00382-019-04622-6

Hirata, F. E., & Grimm, A. M. (2016). The role of synoptic and intraseasonal anomalies in the life cycle of summer rainfall extremes over South America. *Climate Dynamics*, *46*(9–10), 3041–3055. https://doi.org/10.1007/s00382-015-2751-6

Hoell, A., Cannon, F., & Barlow, M. (2018). Middle East and Southwest Asia daily precipitation characteristics associated with the Madden–Julian Oscillation during Boreal Winter. *Journal of Climate*, *31*(21), 8843–8860. https://doi.org/10.1175/JCLI-D-18-0059.1

Huffman, G. J., Bolvin, D. T., Braithwaite, D., Hsu, K., Joyce, R., Xie, P., & Yoo, S.-H. (2015). NASA global precipitation measurement (GPM) integrated multi-satellite retrievals for GPM (IMERG). *Algorithm Theoretical Basis Document*, *4*, 30.

Huffman, G. J., Stocker, E. F., Bolvin, D. T., Nelkin, E. J., & Tan, J. (2019). *GPM IMERG final precipitation L3 1 day 0.1 degree x 0.1 degree V06 [Data set]*. NASA Goddard Earth Sciences Data and Information Services Center. https://doi.org/10.5067/GPM/IMERGDF/DAY/06

IPCC. (2021). *Summary for Policymakers. [in "Climate Change 2021: The Physical Science Basis. Contribution of Working Group I to the Sixth Assessment Report of the Intergovernmental Panel on Climate Change"]*. Cambridge University Press. Retrieved from https://www.ipcc.ch/report/ar6/wg1/downloads/report/IPCC_AR6_WGI_SPM.pdf

Jones, C., & Carvalho, L. M. V. (2012). Spatial–intensity variations in extreme precipitation in the Contiguous United States and the Madden–Julian Oscillation. *Journal of Climate*, *25*(14), 4898–4913. https://doi.org/10.1175/JCLI-D-11-00278.1

Jones, C., Waliser, D. E., Lau, K. M., & Stern, W. (2004). Global occurrences of extreme precipitation and the Madden–Julian Oscillation: Observations and predictability. *Journal of Climate*, *17*(23), 4575–4589. https://doi.org/10.1175/3238.1

Kim, H.-M., Webster, P. J., Toma, V. E., & Kim, D. (2014). Predictability and prediction skill of the MJO in two operational forecasting systems. *Journal of Climate*, *27*(14), 5364–5378. https://doi.org/10.1175/JCLI-D-13-00480.1

Klotzbach, P. J. (2010). On the Madden–Julian oscillation–Atlantic hurricane relationship. *Journal of Climate*, *23*(2), 282–293. https://doi.org/10.1175/2009jcli2978.1

Kossin, J. P., Camargo, S. J., & Sitkowski, M. (2010). Climate modulation of North Atlantic hurricane tracks. *Journal of Climate*, *23*(11), 3057–3076. https://doi.org/10.1175/2010jcli3497.1

Kunkel, K. E., Easterling, D. R., Kristovich, D. A. R., Gleason, B., Stoecker, L., & Smith, R. (2010). Recent increases in U.S. heavy precipitation associated with tropical cyclones. *Geophysical Research Letters*, *37*(24). https://doi.org/10.1029/2010GL045164

Leopold, L. B. (1968). *Hydrology for urban land planning—A guidebook on the hydrologic effects of urban land use* (Vol. 554, p. 26). U.S. Geological Survey. https://doi.org/10.3133/cir554

Maloney, E. D., & Hartmann, D. L. (2000). Modulation of hurricane activity in the Gulf of Mexico by the Madden-Julian oscillation. *Science*, *287*(5460), 2002–2004. https://doi.org/10.1126/science.287.5460.2002

Mansouri, S., Masnadi-Shirazi, M. A., Golbahar-Haghighi, S., & Nazemosadat, M. J. (2021). An analogy toward the real-time multivariate MJO Index to improve the estimation of the impacts of the MJO on the precipitation variability over Iran in the Boreal Cold Months. *Asia-Pacific Journal of Atmospheric Sciences*, *57*(2), 207–222. https://doi.org/10.1007/s13143-020-00188-0

Matthews, A. J., Hoskins, B. J., & Masutani, M. (2004). The global response to tropical heating in the Madden-Julian oscillation during the northern winter. *Quarterly Journal of the Royal Meteorological Society*, *130*(601), 1991–2011. https://doi.org/10.1256/qj.02.123

Mo, K. C. (2000). The association between intraseasonal oscillations and tropical storms in the Atlantic basin. *Monthly Weather Review*, *128*(12), 4097–4107. https://doi.org/10.1175/1520-0493(2000)129<4097:tabioa>2.0.co;2

Mundhenk, B. D., Barnes, E. A., Maloney, E. D., & Baggett, C. F. (2018). Skillful empirical subseasonal prediction of landfalling atmospheric river activity using the Madden–Julian oscillation and quasi-biennial oscillation. *Npj Climate and Atmospheric Science*, *1*(1), 7. https://doi.org/10.1038/s41612-017-0008-2

Nazemosadat, M. J., & Shahgholian, K. (2017). Heavy precipitation in the southwest of Iran: Association with the Madden–Julian Oscillation and synoptic scale analysis. *Climate Dynamics*, *49*(9), 3091–3109. https://doi.org/10.1007/s00382-016-3496-6

Nazemosadat, M. J., Shahgholian, K., Ghaedamini, H., & Nazemosadat, E. (2021). Introducing new climate indices for identifying wet/dry spells within an Madden-Julian Oscillation phase. *International Journal of Climatology*, *41*(S1). https://doi.org/10.1002/joc.6799

Prat, O. P., & Nelson, B. R. (2013a). Mapping the world's tropical cyclone rainfall contribution over land using the TRMM Multi-satellite Precipitation Analysis: World's Tropical Cyclone Rainfall Contribution. *Water Resources Research*, *49*(11), 7236–7254. https://doi.org/10.1002/wrcr.20527

Prat, O. P., & Nelson, B. R. (2013b). Precipitation contribution of tropical cyclones in the Southeastern United States from 1998 to 2009 using TRMM satellite data. *Journal of Climate*, *26*(3), 1047–1062. https://doi.org/10.1175/JCLI-D-11-00736.1

Prat, O. P., & Nelson, B. R. (2016). On the link between tropical cyclones and daily rainfall extremes derived from global satellite observations. *Journal of Climate*, *29*(17), 6127–6135. https://doi.org/10.1175/JCLI-D-16-0289.1

Prat, O. P., & Nelson, B. R. (2020). Satellite precipitation measurement and extreme rainfall. In V. Levizzani, C. Kidd, D. B. Kirschbaum, C. D. Kummerow, K. Nakamura, & F. J. Turk (Eds.), *Satellite precipitation measurement* (Vol. 69, pp. 761–790). Springer International Publishing. https://doi.org/10.1007/978-3-030-35798-6_16

Ralph, F. M., Neiman, P. J., Kiladis, G. N., Weickmann, K., & Reynolds, D. W. (2011). A multiscale observational case study of a Pacific atmospheric river exhibiting tropical–extratropical connections and a mesoscale frontal wave. *Monthly Weather Review*, *139*(4), 1169–1189. https://doi.org/10.1175/2010MWR3596.1

Riddle, E. E., Stoner, M. B., Johnson, N. C., L'Heureux, M. L., Collins, D. C., & Feldstein, S. B. (2013). The impact of the MJO on clusters of wintertime circulation anomalies over the North American region. *Climate Dynamics*, *40*(7–8), 1749–1766. https://doi.org/10.1007/s00382-012-1493-y

Saha, S., Moorthi, S., Pan, H.-L., Wu, X., Wang, J., Nadiga, S., et al. (2010). The NCEP climate forecast system reanalysis. *Bulletin of the American Meteorological Society*, *91*(8), 1015–1057. https://doi.org/10.1175/2010BAMS3001.1

Saha, S., Moorthi, S., Wu, X., Wang, J., Nadiga, S., Tripp, P., et al. (2014). The NCEP climate forecast system version 2. *Journal of Climate*, *27*(6), 2185–2208. https://doi.org/10.1175/JCLI-D-12-00823.1

Shimizu, M. H., Ambrizzi, T., & Liebmann, B. (2017). Extreme precipitation events and their relationship with ENSO and MJO phases over northern South America: Extreme events in ENSO and MJO phases over Northern South America. *International Journal of Climatology*, *37*(6), 2977–2989. https://doi.org/10.1002/joc.4893

Vitart, F., & Molteni, F. (2010). Simulation of the Madden– Julian Oscillation and its teleconnections in the ECMWF forecast system. *Quarterly Journal of the Royal Meteorological Society*, *136*(649), 842–855. https://doi.org/10.1002/qj.623

Wheeler, M. C., & Hendon, H. H. (2004). An all-season real-time multivariate MJO index: Development of an index for monitoring and prediction. *Monthly Weather Review*, *132*(8), 1917–1932. https://doi.org/10.1175/1520-0493(2004)132<1917:aarmmi>2.0.co;2

Wilks, D. S. (2006). On "Field Significance" and the False Discovery Rate. *Journal of Applied Meteorology and Climatology*, *45*(9), 1181–1189. https://doi.org/10.1175/JAM2404.1

Zhang, C. (2005). Madden-Julian Oscillation. *Reviews of Geophysics*, *43*, RG2003., https://doi.org/10.1029/2004RG000158

Zhang, C. (2013). Madden-Julian Oscillation: Bridging weather and climate. *Bulletin of the American Meteorological Society*, *94*, 1849–1870. https://doi.org/10.1175/BAMS-D-12-00026.1

Zhang, C., Gottschalck, J., Maloney, E. D., Moncrieff, M. W., Vitart, F., Waliser, D. E., et al. (2013). Cracking the MJO nut. *Geophysical Research Letters*, *40*(6), 1223–1230. https://doi.org/10.1002/grl.50244